Supporting Information for:

Ping–Pong Energy Transfer in a Bodipy-Containing Pt(II)–Schiff Base Complex: Synthesis, Photophysical Studies, and Anti-Stokes Shift Increase in Triplet–Triplet Annihilation Upconversion

Syed S. Razi,[a§] *Yun Hee Koo,*[b§] *Woojae Kim,*[b] *Wenbo Yang,*[a] *Zhijia Wang,*[a] *Habtom Gobeze,*[c] *Francis D'Souza*,[c] *Jianzhang Zhao*[a]* and *Dongho Kim*[b]*

[a] State Key Laboratory of Fine Chemicals, School of Chemical Engineering, Dalian University of Technology, E–208 West Campus, 2 Ling Gong Rd., Dalian 116024, P. R. China.

E–mail: zhaojzh@dlut.edu.cn

[b] Spectroscopy Laboratory for Functional π–Electronic Systems, and Department of Chemistry, Yonsei University, Seoul 120–749, Korea; E–mail: dongho@yonsei.ac.kr

[c] Department of Chemistry, University of North Texas, 1155 Union Circle, #305070, Denton, TX 76203-5017, USA.

Index

Synthesis and Characterization. *Synthesis of **1**.* 3, 5-di-*tert*-butyl-2 hydroxybenzaldehyde (936 mg, 4.0 mmol) was dissolved in EtOH (30 mL), 4-bromo-phenylenediamine (374 mg, 2.0 mmol) and acetic acid (0.5 mL) was added, the mixture was refluxed for 10 h until the reaction have completed (monitored by TLC). After completed the reaction, solvent was evaporated under reduced pressure, washed with water, dried in air and recrystallized from EtOH to give orange needle crystals (1.6 g, 3.47 mmol) in 84.6% yield. ^{1}H NMR (400 MHz, DMSO–d_6): δ 13.67 (s, 1H), 13.57 (s, 1H), 9.03 (s, 1H), 8.98 (s, 1H), 7.80 (s, 1H,), 7.60 (s, 1H,), 7.53 (s, 1H,), 7.50–7.47 (d, 2H, J = 5.2 Hz), 7.41 (t, 2H, J = 3.2 Hz), 1.38 (s, 18H), 1.29 (s, 18H). MALDI–HRMS: calcd ($[C_{36}H_{47}BrN_2O_2]^+$), m/z = 618.2821, found m/z = 619.2925$(m+H)^+$.

*Synthesis of **2**.* K_2PtCl_4 (415 mg, 1.0 mmol), **1** (619 mg, 1.0 mmol) and K_2CO_3 (414 mg, 3.0 mmol) were dissolved in degassed DMSO (10 mL), the flask was vacuumed and back–filled with argon for several times, then the mixture was stirred at 75 °C for 12 h. The red precipitation was collected and further purified by column chromatography (dichloromethane as eluent). After removal of the solvent the red solid (450.5 mg, 0.77 mmol) was collected in 60.6% yield. ^{1}H NMR (400 MHz, DMSO–d_6): δ 9.59 (s, 1H), 9.54 (s, 1H), 8.77 (s, 1H,), 8.45 (s, 1H,), 7.73 (d, 2H, J = 12.0 Hz), 7.66 (d, 1H, J = 8.0 Hz,), 7.61 (t, 2H, J_1 = 2.4 Hz, J_2 = 2.4 Hz), 1.51 (s, 18H), 1.33 (s, 18H). MALDI–MS: calcd ($[C_{36}H_{45}BrN_2O_2Pt]^+$), m/z = 811.2312, found m/z = 811.2197.

*Synthesis of **4**.* Under an Ar atmosphere, 4–formylbenzeneboronic acid (1.50 g, 10.0 mmol) and pinacol (1.18 g, 10 mmol) were placed with toluene (150 mL) in a round-bottom flask.

The mixture was refluxed for 12 h at 120 °C. Evaporation of the solvent under reduced pressure lead to formation of a white–yellow solid **3** (2.3 g, yield: 99%). This crude product was used for the next step of the synthesis without further purification. Under an Ar atmosphere, the above crude product **3** (2.0 g, 8.7 mmol) and 2,4–dimethylpyrrole (2 mL, 20 mmol) were dissolved in dry CH_2Cl_2 (150 mL). A few drops of trifluoroacetic acid were added to the solution, and the mixture was stirred 12 h at room temperature. After completion of the reaction (monitored via TLC), a solution of DDQ (2.0 g, 8.7 mmol) in freshly distilled THF was added to the reaction mixture. The reaction mixture was stirred for 2 h. Absolute triethylamine (10 mL) was added to the reaction mixture. After this mixture was stirred for 15 min, $BF_3{\cdot}Et_2O$ (10 mL) was added dropwise under ice cold conditions. After the reaction mixture was stirred for 2 h more, the mixture was washed with water several times and then extracted with DCM. The organic phase was dried over anhydrous Na_2SO_4, and then the solvent was evaporated under reduced pressure. The residue was purified with column chromatography (silica gel, CH_2Cl_2) to give a red solid (1.2 g, yield 31%). ^{1}H NMR ($CDCl_3$, 500 MHz): δ 7.91 (d, 2H, J = 5.0 Hz), 7.30 (d, 2H, J = 5.0 Hz), 5.97 (s, 2H), 2.55 (s, 6H), 1.39 (s, 12H), 1.37 (s, 6H). TOF MALDI–HRMS: calcd ($[C_{25}H_{30}N_2O_2B_2F_2]^+$), m/z = 450.2462, found m/z = 450.2446.

Table S1. Crystal Data Collection Parameters for the Pt–Ph Complex

Complexes	**Pt–Ph**
Sum Formula	$C_{42}H_{50}N_2O_2Pt$
M (g mol^{-1})	809.93
Temp / K	296 (2)
Crystal System	Orthorhombic
Space group	P_{bcn}
a (Å)	17.316
b (Å)	30.680
c (Å)	14.133
α (deg)	90
β (deg)	90
γ (deg)	90
Volume / Å^3	7508
Z	8
D_{calc} / g.cm^{-3}	1.433
Crystal size (mm)	0.23 × 0.12 × 0.09
F (000)	3280
μ (Mo – Kα) / mm^{-1}	3.774
θ (deg)	2.29 – 19.15
Reflections collected	6623
Independent reflections	35401
Parameters	437
Largest diff. peak and hole (e Å^{-3})	0.23, 0.09
Goodness of fit	0.984
R^a	0.0582[b]
$\omega R_2{}^a$	0.1386 [b]

[a] $R = \sum \| |F_o| - |F_c| \| / \sum |F_o|$, $wR_2 = \left[\sum \left(w\left(F_o^2 - F_c^2 \right)^2 \right) / \sum \left(w\left(F_o^2 \right)^2 \right) \right]^{1/2}$; $\left[F_o > 4\sigma\left(F_o \right) \right]$. [b]

Based on all data.

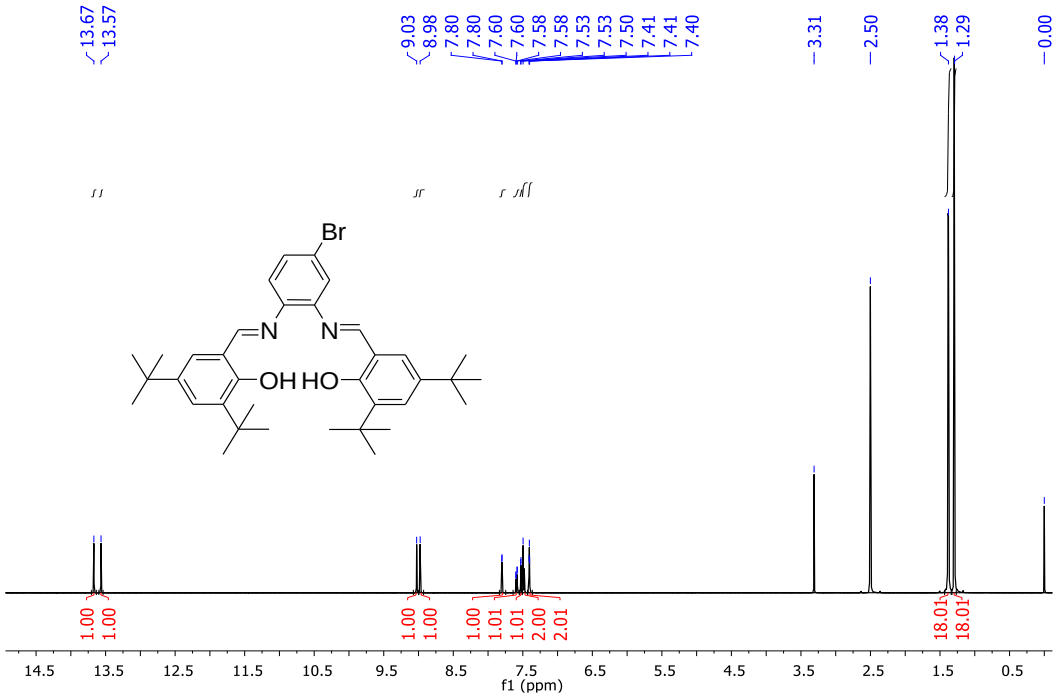

Figure S1. ^{1}H NMR spectrum of compound **1** (400 MHz, DMSO-d_6), 25 °C.

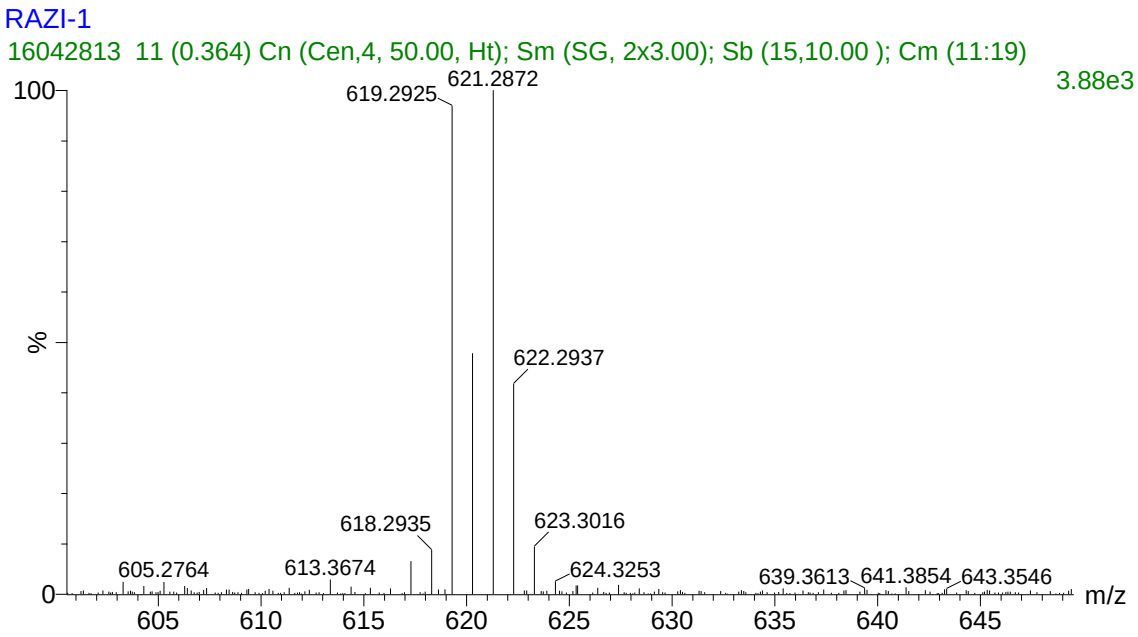

Figure S2. TOF-HR mass spectrum of compound **1**.

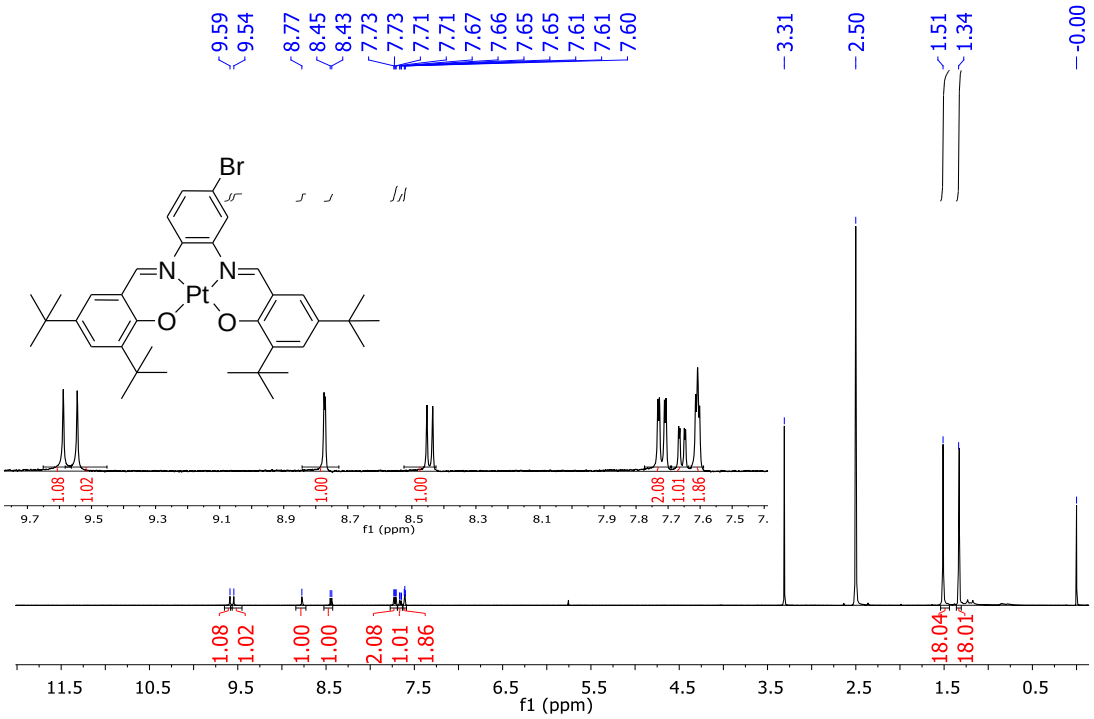

Figure S3. ^{1}H NMR spectrum of compound **2** with partial enlarged details (400 MHz, DMSO-d_6), 25 °C.

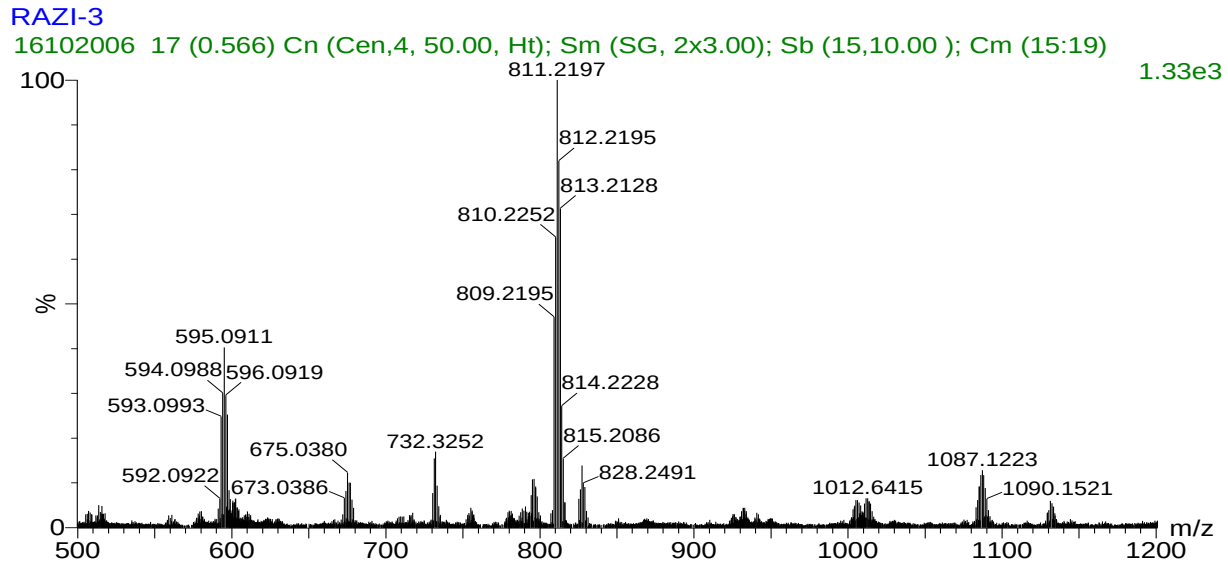

Figure S4. MALDI–TOF–HR mass spectrum of compound **2**.

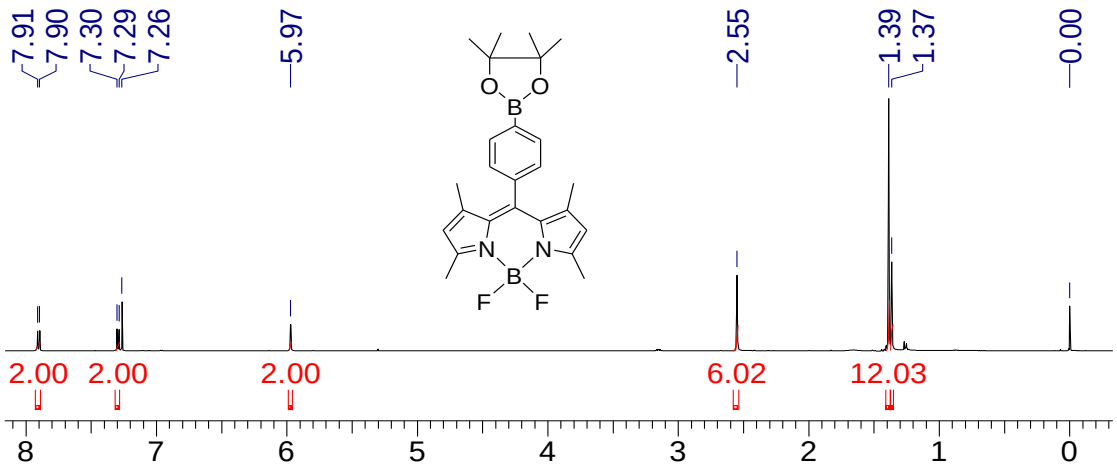

Figure S5. ^{1}H NMR spectrum of compound **4** (400 MHz, $CDCl_3$), 25 °C.

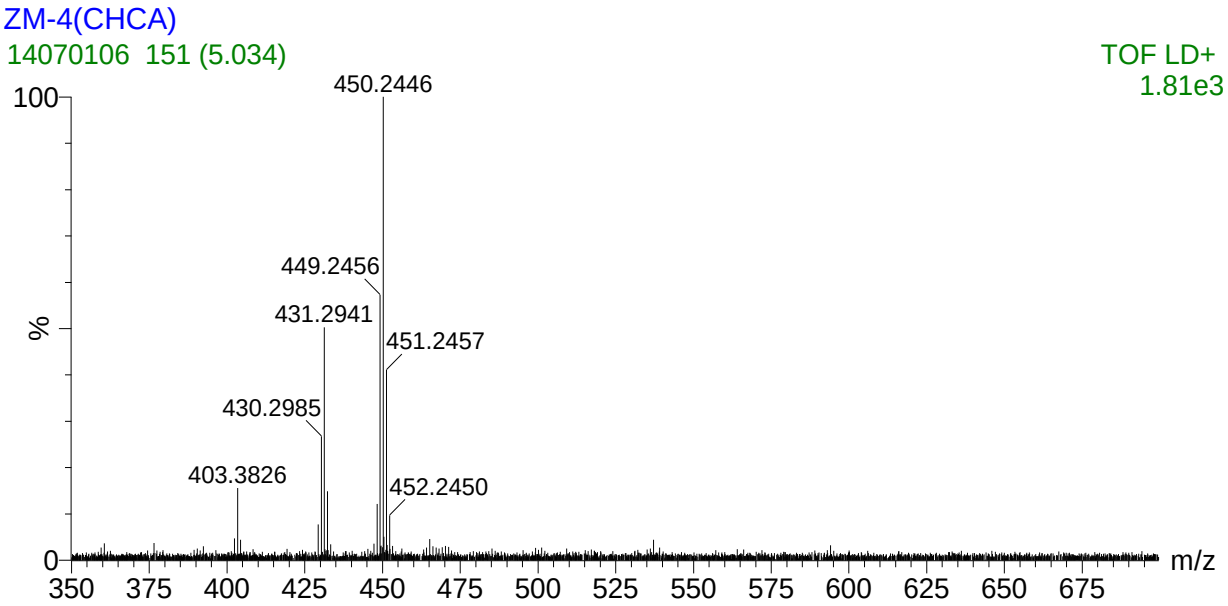

Figure S6. MALDI–TOF–HR mass spectrum of compound **4**.

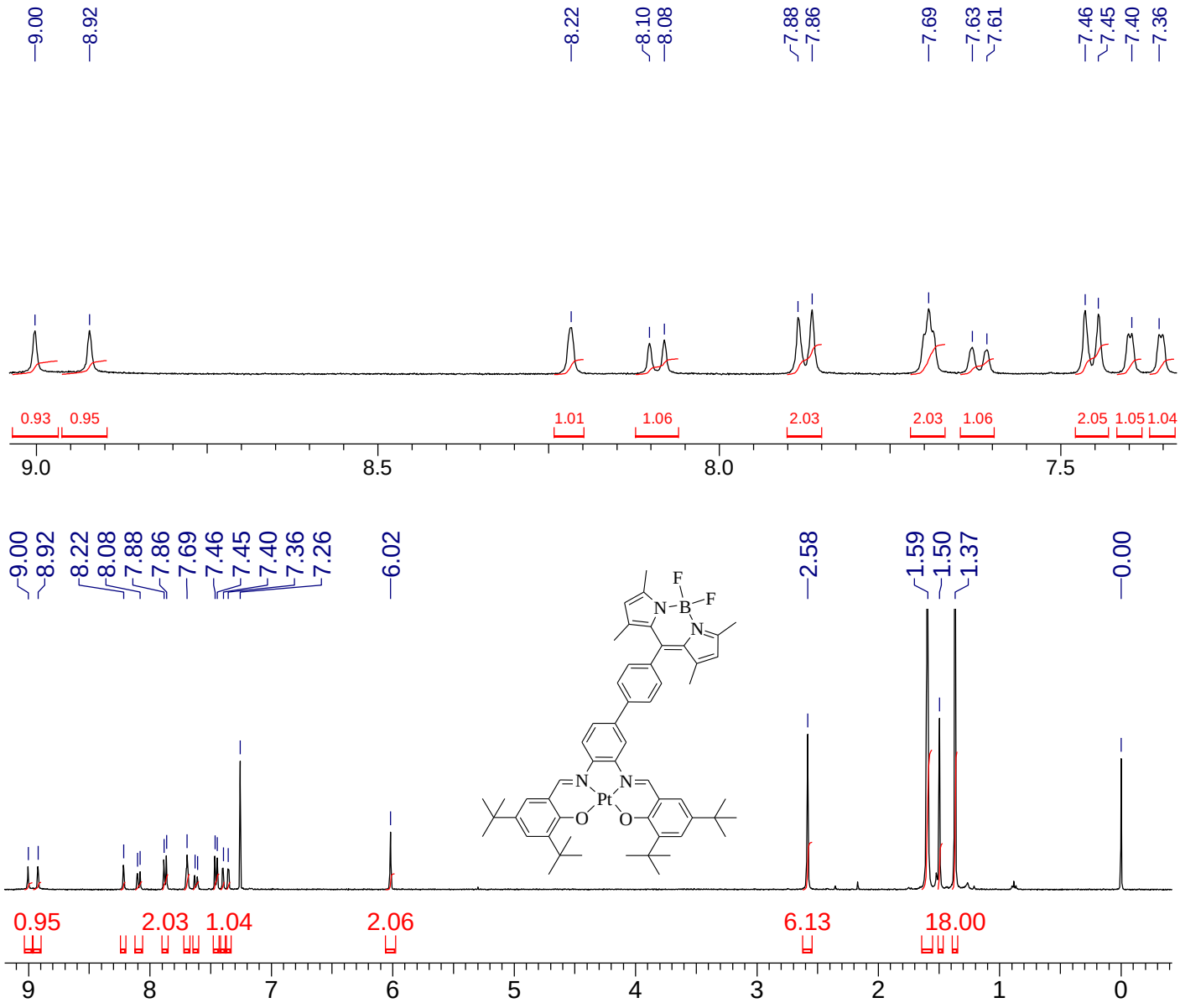

Figure S7. ^{1}H NMR spectrum of compound **Pt–BDP** with partial enlarged details (400 MHz, $CDCl_3$), 25 °C.

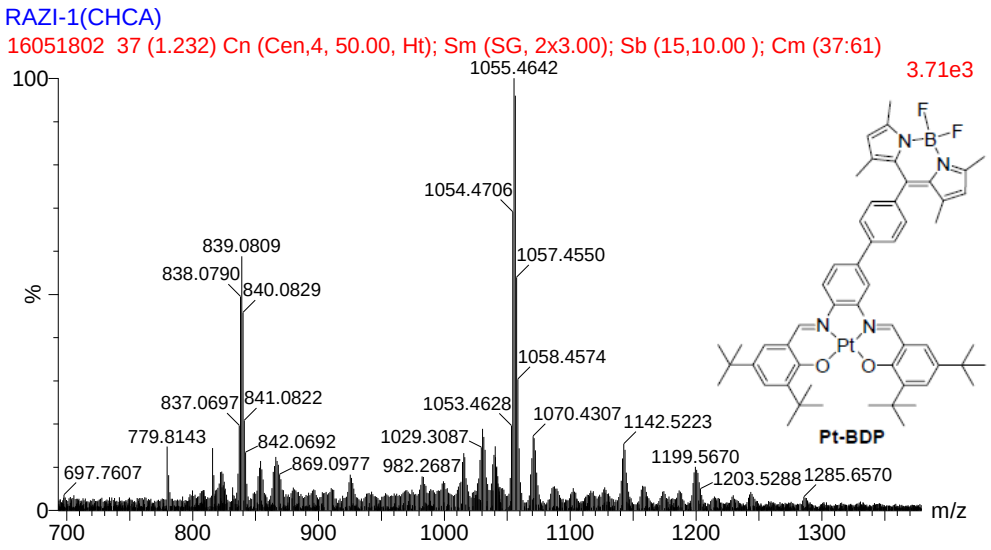

Figure S8. MALDI–TOF–HR mass spectrum of compound **Pt–BDP**.

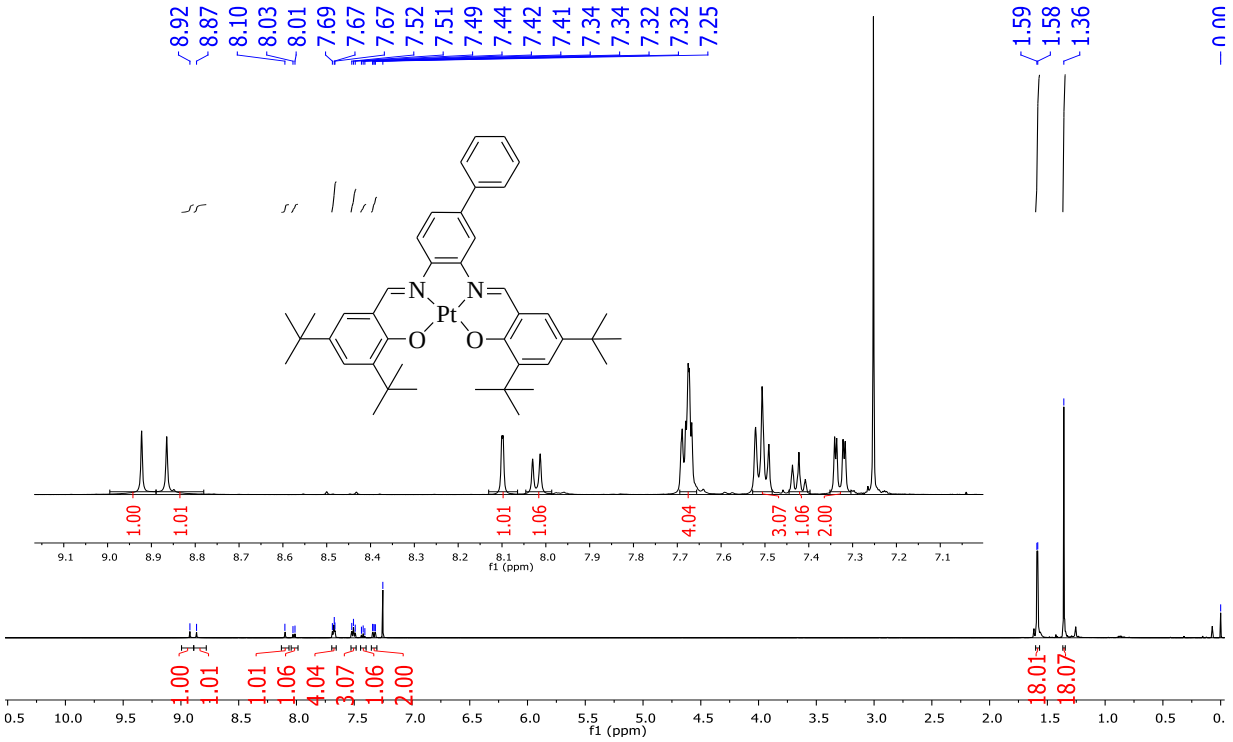

Figure S9. ^{1}H NMR spectrum of compound **Pt–Ph** with partial enlarged details (400 MHz, $CDCl_3$), 25 °C.

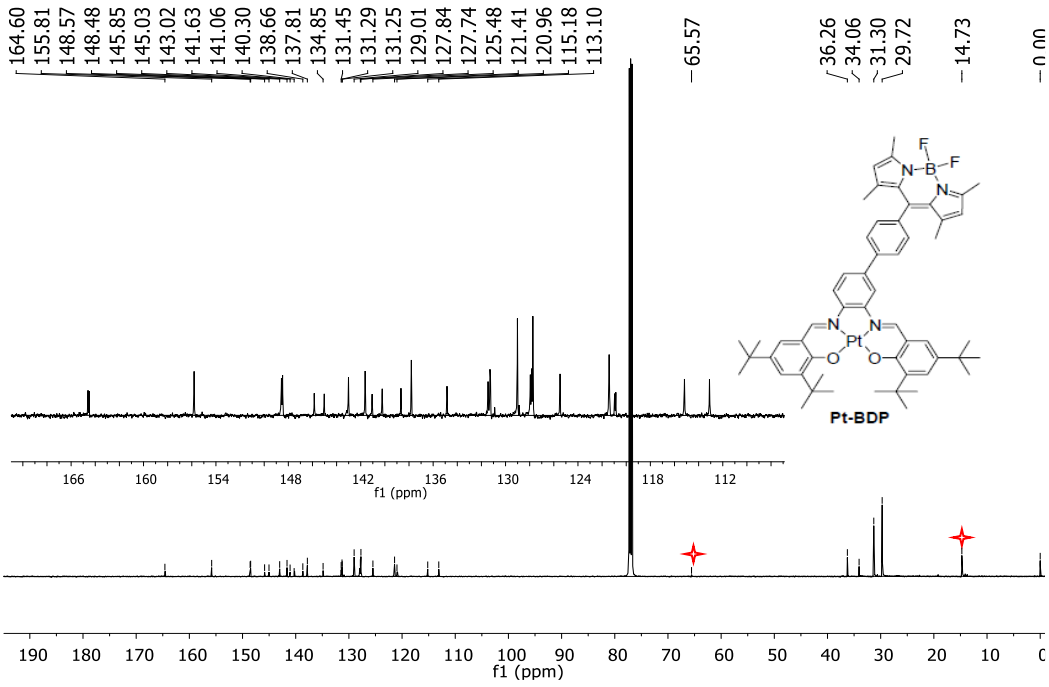

Figure S10. ^{13}C NMR spectrum of compound **Pt–BDP** with partial enlarged details (100 MHz, $CDCl_3$), 25 °C. The asterisks indicated solvent peak of ether.

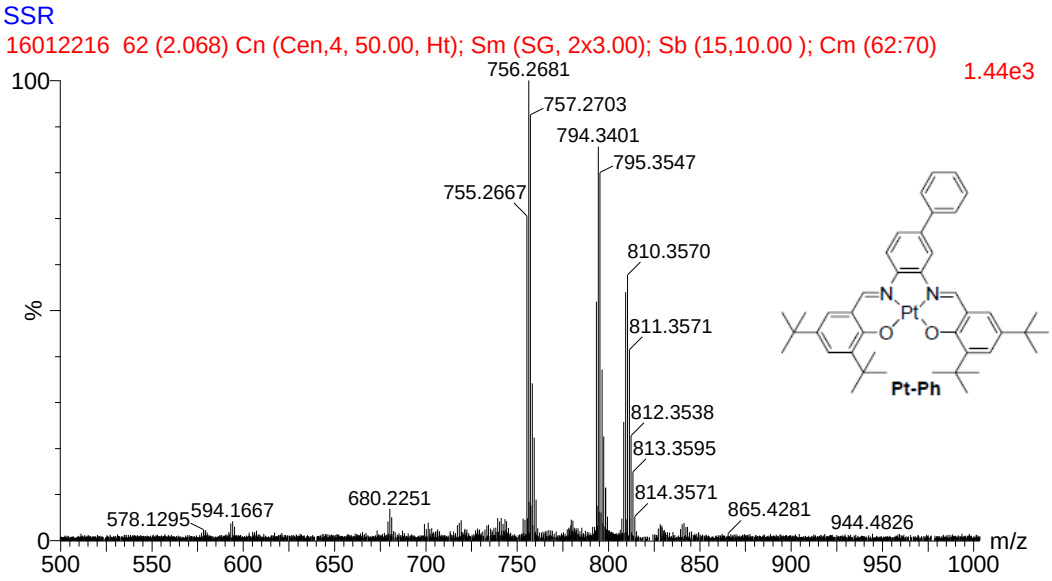

Figure S11. MALDI–TOF–HR mass spectrum of compound **Pt–Ph**.

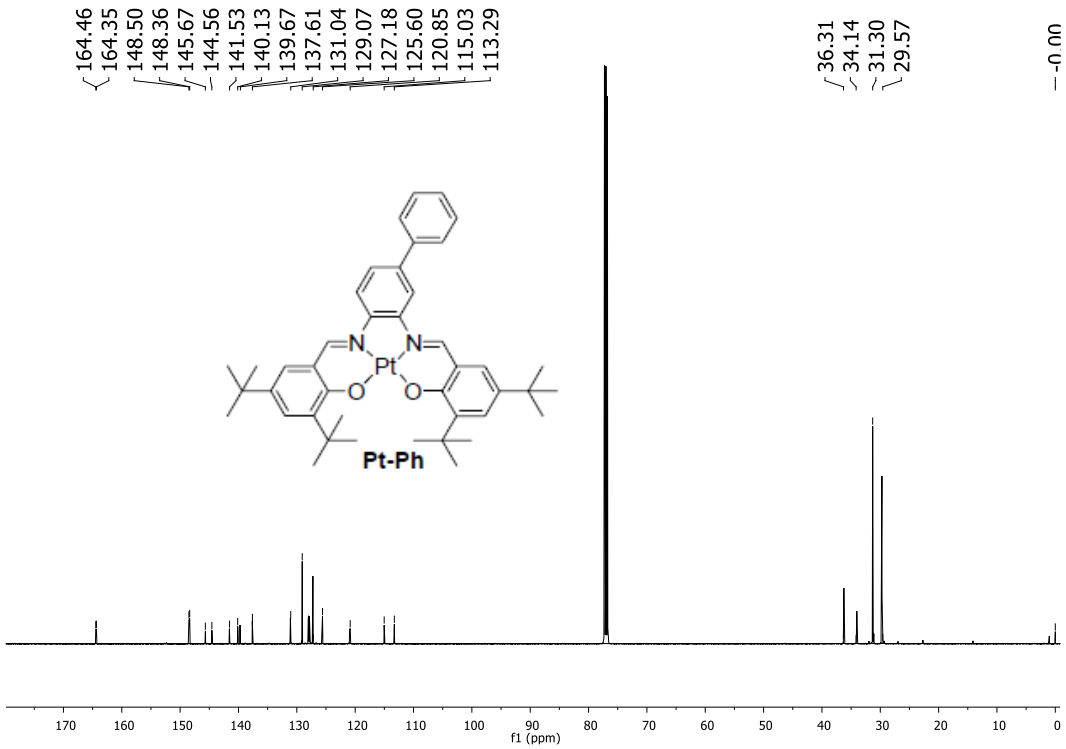

Figure S12. ^{13}C NMR spectrum of compound **Pt–Ph** (100 MHz, $CDCl_3$), 25 °C.

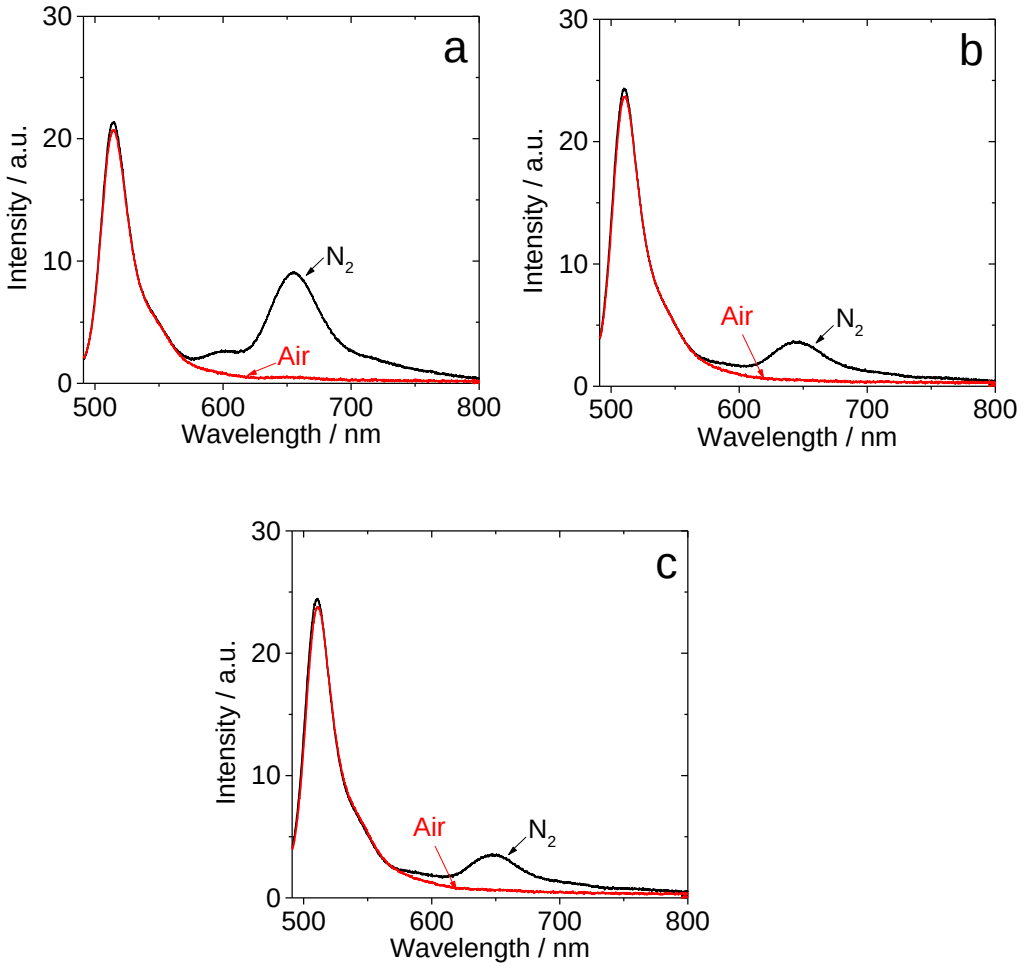

Figure S13. Photoluminescence spectra of **Pt–BDP** in different solvents (a) CH_2Cl_2, (b) CH_3CN and (c) CH_3OH under air and N_2 atmosphere. λ_{ex} = 475 nm. c = 1.0×10^{-5} M. 20 °C.

Note we found **Pt-BDP** is unstable toward photo-irradiation, the resulted decomposition may induce a stronger emission at 515 nm. However, for the above results in Figure S13, we confirmed that the samples are pure, and the phosphorescence emission band becomes weaker in polar solvents. With the same sample (solution), we reproduced the results in toluene (Figure 2b in the main text of the manuscript).

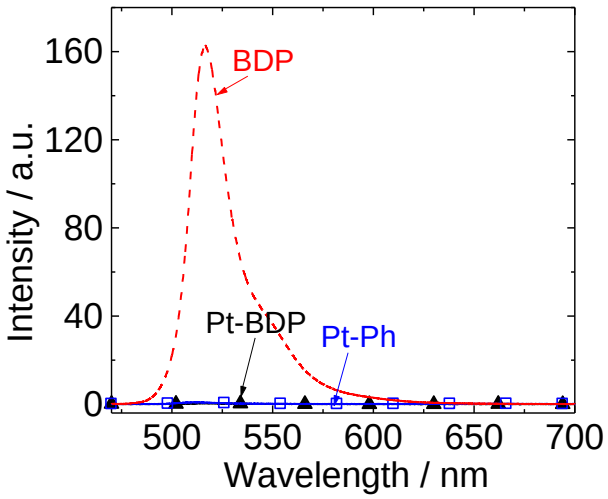

Figure S14. Luminescence spectra of **Pt–BDP**, **Pt–Ph** and **BDP**. Determined with optically matched solution (λ_{ex} = 475 nm). c = ca. 1.0×10^{-5} M in toluene. 20 °C.

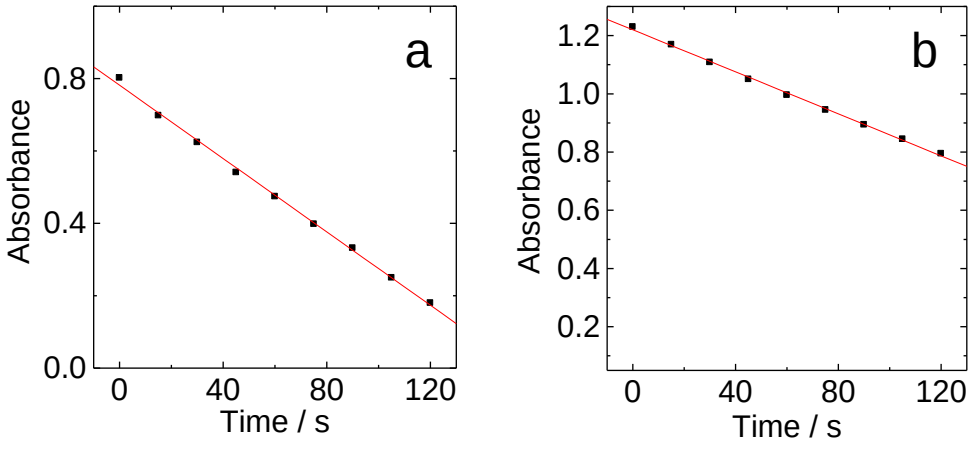

Figure S15. Singlet oxygen ($^1O_2$) photosensitizing of (a) **Pt–BDP** (λ_{ex} = 500 nm). c = 1.0 × 10^{-5} M and (b) **Pt–Ph**, Xenon lamp was used as light source. (λ_{ex} = 500 nm, optically matched solutions were used), c = 1.0 × 10^{-5} M. In toluene. 20 °C.

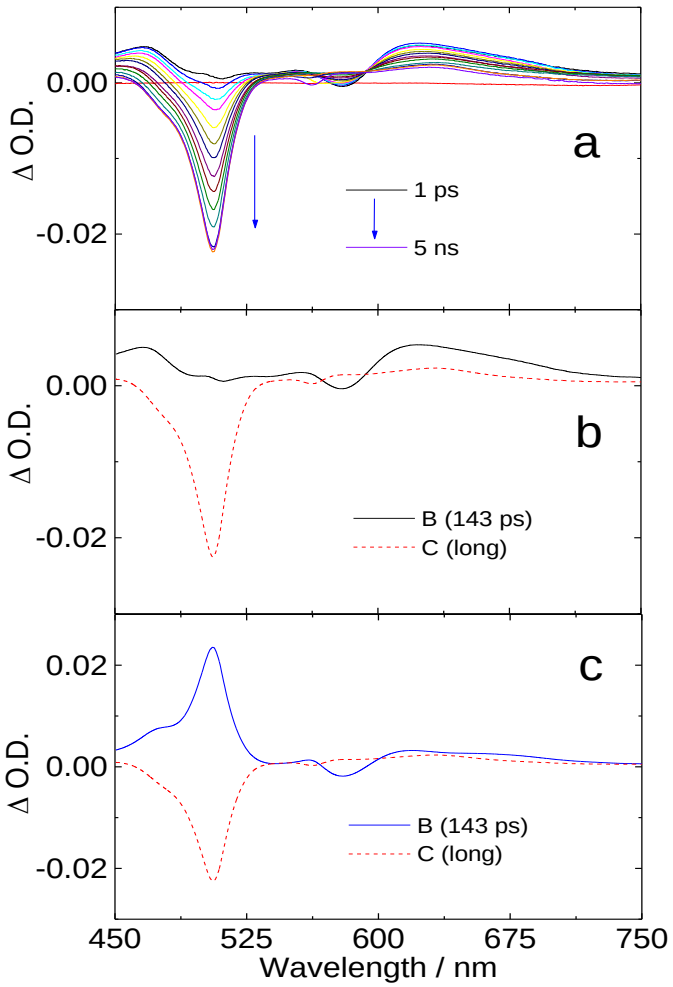

Figure S16. Femtosecond transient absorption spectra measured (a) from 1 ps to 5 ns and (b) Evolution-Associated and (c) Decay-Associated Difference Spectra of **Pt–BDP** in toluene obtained from global target analysis at 560 nm excitation.

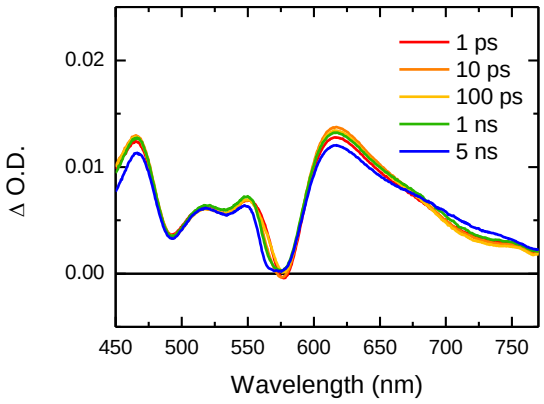

Figure S17. Femtosecond transient absorption spectra measured from 1 to 5 ns of **Pt-Ph** in toluene. 560 nm excitation)

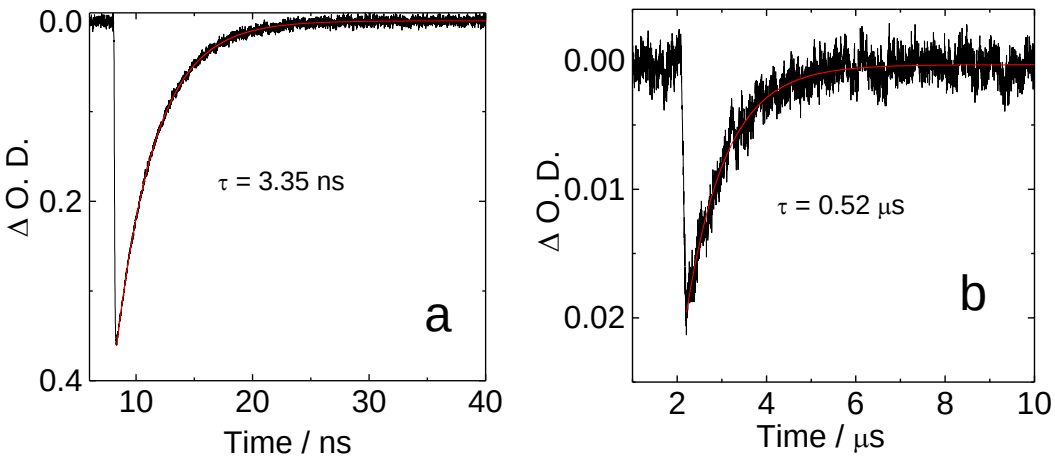

Figure S18. The nanosecond time–resolved transient difference absorption spectra. (a) **Pt–BDP** and (b) **Pt–Ph** in aerated toluene. λ_{ex} = 532 nm laser, 20°C.

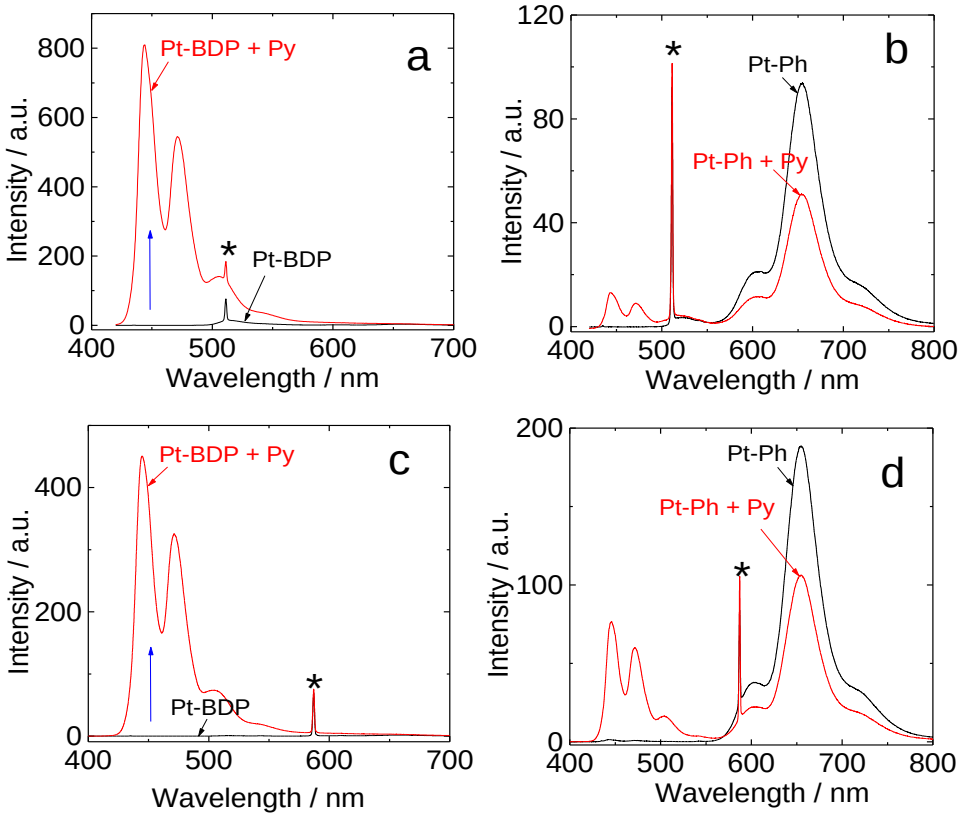

Figure S19. Comparable TTA upconversion with (a) **Pt**–**BDP** and (b) **Pt**–**Ph** at 510 nm laser in toluene. For (c) **Pt**–**BDP** and (d) **Pt**–**Ph** at 589 nm laser as the triplet sensitizers (c = 1.0×10^{-5} M) and perylene as the acceptor (4.0×10^{-5} M) in optically matched toluene solution. The asterisks indicate the scattered laser. Excited with CW laser (λ_{ex} = 510 and 589 nm), 4 mW, 20 °C.

Table S2. Properties of the Low-Lying Electronic Excited States of Pt–BDP Calculated by TDDFT//B3LYP/GENECP, based on the DFT//B3LYP/GENECP-Optimized Ground-State Geometries.

	Electronic transition	Energy / eV/nm [a]	f [b]	Composition [c]	CI [d]	Character
Singlet	$S_0 \rightarrow S_1$	2.29 / 542	0.1592	H→L+1	0.6938	ILCT
	$S_0 \rightarrow S_6$	2.86 / 433	0.5827	H–1→L	0.6937	ILCT
	$S_0 \rightarrow S_9$	3.20 / 387	0.3539	H–2→L+2	0.6618	ILCT
	$S_0 \rightarrow S_{10}$	3.23 / 384	0.7775	H–2→L+2	0.6618	ILCT
Triplet [e]	$S_0 \rightarrow T_1$	1.52 / 815	0.0000	H–1→L	0.7085	MLCT
	$S_0 \rightarrow T_2$	1.84 / 673	0.0000	H–2→L+2	0.6653	MLCT/ILCT
	$S_0 \rightarrow T_3$	2.01 / 617	0.0000	H–2→L+1	0.5425	MCT/ILCT

[a] Only the selected low-lying excited states are presented. [b] Oscillator strengths. [c] Only the main configurations are presented. [d] The CI coefficients are in absolute values. [e] No spin-orbital coupling effect is considered; thus, the oscillator strength, i.e. the *f* values, are zero.